On-Demand Routing and Spectrum Allocation for Energy-Efficient AoD Nodes in SDM-EONs

Shohei Fujii, Yusuke Hirota, Hideki Tode, and Takashi Watanabe

***Abstract*—Elastic optical networks (EONs) and space-division multiplexing (SDM) are promising technologies for future core optical networks with high transmission capacity. Traditional optical node architectures for SDM-EONs have two important problems: flexibility and power consumption. Architecture on demand (AoD) is a new concept for an optical node architecture, and an optical node based on this concept is called an AoD node. AoD nodes can be dynamically constructed according to the traffic request by interconnecting input/output ports and building modules with optical switches. Although AoD nodes have great flexibility, power consumption is still a serious problem for them. In this paper, we propose an energy-efficient network system that includes a novel energy-efficient AoD node architecture and resource assignment method cooperating with this node architecture. The proposed system solves the power-consumption problem by simplifying the implemented building modules based on spatial multiplicity of SDM-EONs. The proposed on-demand routing and spectrum allocation method efficiently satisfies the restricted spectrum arrangement that is required by energy-efficient AoD nodes. Finally, we evaluate the proposed system of node architecture and resource allocation method through computer simulations. The simulations show that the proposed network system can improve both the power consumption and the blocking probability of path setup requests in the entire network.**

***Index Terms*—Architecture on demand; Elastic optical network; Routing and spectrum allocation; Space division multiplexing.**

I. Introduction

Expansion of the transmission capacity of core optical networks is necessary because Internet traffic is rapidly increasing. The technologies of elastic optical networks (EONs) have been studied, and the utilization efficiency of core optical networks has been improved compared to that of traditional wavelength division multiplexing (WDM) networks [1–3]. However, the transmission capacity of an existing single-mode single-core optical fiber is reaching its physical limit owing to the improved high utilization of network resources. Optical fibers based on space-division multiplexing (SDM) technologies are important novel transmission devices that can expand the transmission capacity of core optical networks beyond the physical limit of traditional optical fibers [4–6]. The appearance of SDM-based optical fibers and an increase in the number of underlying optical fibers, which are aimed at expanding transmission capacity of optical networks, are expected to enlarge and complicate optical switching nodes in future core optical networks. Broadcast-and-select and spectrum-routing are general optical switching node architectures that have enough flexibility to realize optical networks that are fully elastic [7,8]. In these architectures, the spectrum selective switch (SSS) is not only the main building module but also the dominant module in terms of power consumption. When optical switching nodes become complex and large-scale, cascaded SSSs dramatically increase the power consumption of these optical switching nodes, owing to the limited port count of SSSs [9].

To suppress the increase in the number of building modules, a hierarchical optical switching node architecture using small optical cross connects (OXCs) as subsystem modules has been proposed [10]. This hierarchical node architecture divides the switching component into subsystems of smaller OXCs and suppresses the increase in the number of cascaded SSSs and erbium-doped fiber amplifiers (EDFAs). On the other hand, their partially restricted switching negatively affects the transmission success rate, and there is a trade-off between suppression of the modular cost and the transmission success rate. Therefore, it is necessary to establish a completely different node architecture to achieve cost reduction and successful transmission. Reference [11] also reduces the number of building modules implemented in optical nodes by introducing a completely different novel optical node architecture called an architecture on demand (AoD) node. In AoD nodes, an optical backplane, which is usually implemented using a large-port-count three-dimensional microelectromechanical system (3D-MEMS), interconnects input/output ports and building modules in an arbitrary manner, as shown in Fig. 1. Use of an AoD node can reduce the number of building modules by supplying just enough signal switching and/or processing because these interconnections are dynamically constructed according to the request. In other words, the AoD concept requires an

Manuscript received March 14, 2017; revised July 27, 2017; accepted August 26, 2017; published October 11, 2017 (Doc. ID 290604).

S. Fujii (e-mail: fujii.shohei@ist.osaka-u.ac.jp), Y. Hirota, and T. Watanabe are with the Department of Information Networking, Graduate School of Information Science and Technology, Osaka University, Osaka, Japan.

H. Tode is with the Graduate School of Engineering, Osaka Prefecture University, Osaka, Japan.

https://doi.org/10.1364/JOCN.9.000960

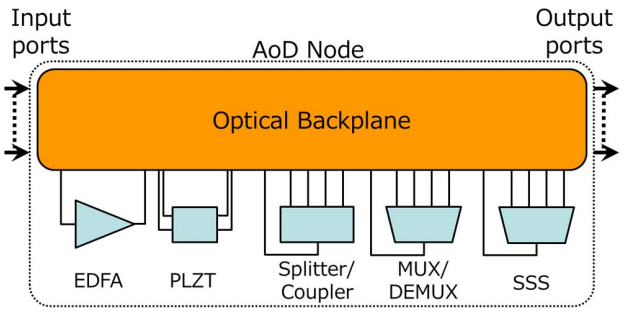

Fig. 1. Basic architecture of AoD nodes [11].

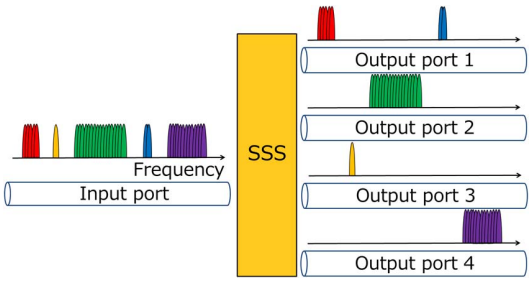

Fig. 2. Concept of the SSS.

appropriate resource allocation method (which creates an appropriate switching request) considering these interconnections in AoD nodes.

In this paper, we propose a novel energy-efficient network system that consists of a novel node architecture and resource assignment method considering an AoD node architecture in SDM-EONs. First, we discuss the proposal of energy-efficient AoD node architecture that can reduce power consumption of AoD nodes. This proposed node architecture requires partially restricted spectrum allocation to adopt low-power-consumption building modules. Then, we also propose a novel on-demand resource allocation method suited for our proposed energy-efficient AoD nodes. The proposed resource allocation method simultaneously reduces the blocking probability of path setup requests in the entire network because its allocation policy reduces spectrum fragmentation. Therefore, our proposed AoD node architecture and on-demand resource allocation method can improve both the power consumption and the blocking probability in EONs. There are three main contributions in this paper. The first contribution is a novel energy-efficient optical node architecture based on the AoD concept. The second contribution is a new resource assignment method realizing energy-efficient AoD nodes by appropriately arranging spectra. The third contribution is improving the power consumption and blocking rate of connections in SDM-EONs.

The rest of this paper is organized as follows. Section II introduces optical node architectures for EONs, including both traditional static node architectures and an AoD node architecture. Section III explains our proposed energy-efficient AoD node architecture, which incorporates low-power-consumption modules. Section IV proposes an on-demand routing and spectrum allocation method suitable for the energy-efficient AoD node architecture. Section V evaluates the performance of the proposed method. Section VI concludes this paper.

II. Optical Node Architecture for EONs

A. Traditional Optical Node Architectures for EONs

In EONs, the optical switching nodes need to handle transmission signals with greater flexibility and finer granularity than in traditional WDM networks. The SSS, which is also called the bandwidth variable wavelength selective switch of a flexible WSS, is the most important building module in the optical nodes of EONs [2]. The SSS can filter spectra with an arbitrary width from input signals and switch them to arbitrary ports without signal replication, as shown in Fig. 2. The flexibility of spectrum selection in the SSS realizes flexible networking in EONs.

Figure 3 shows traditional optical node architectures based on SSSs for EONs [7,8]. In the broadcast-and-select architecture, the input signals are replicated in splitters and broadcast to all output ports. On each output port, the appropriate spectra are selected using an SSS, and the multiplexed signal is transmitted through the output port. However, the replication by these splitters seriously degrades the transmission signals when the scale of a node is large [12,13]. In the spectrum-routing architecture, the input signals are first demultiplexed by an ingress SSS without replication. Then, these demultiplexed signals are routed to different output ports and finally combined, also by an egress SSS, at the output port. The spectrum-routing architecture does not produce signal degradation by splitters, unlike the broadcast-and-select architecture, but the spectrum-routing architecture is more costly than the broadcast-and-select architecture because the number of SSSs is doubled.

In both architectures, the cost of optical nodes is a serious problem. When the number of input/output ports of an optical node is large, e.g., because multicore fibers (MCFs) are adopted, SSSs with the same port count are required in these traditional node architectures. However, the port count of an SSS has a physical limit, e.g., 20 for a current commercial SSS. If traditional node architectures require a higher port count than this limit, cascaded SSSs are usually implemented for these architectures, explosively increasing the number of required SSSs for optical nodes. (See Appendix A for more information on the number of required SSSs.) Therefore, other optical node architecture is required to mitigate the cost increase due to the use of cascaded SSS.

B. AoD Nodes

The AoD concept was introduced mainly as a solution to the problem of limited flexibility in traditional node architectures due to the hard-wired arrangement of modules [11]. The optical backplane in AoD nodes (Fig. 1)

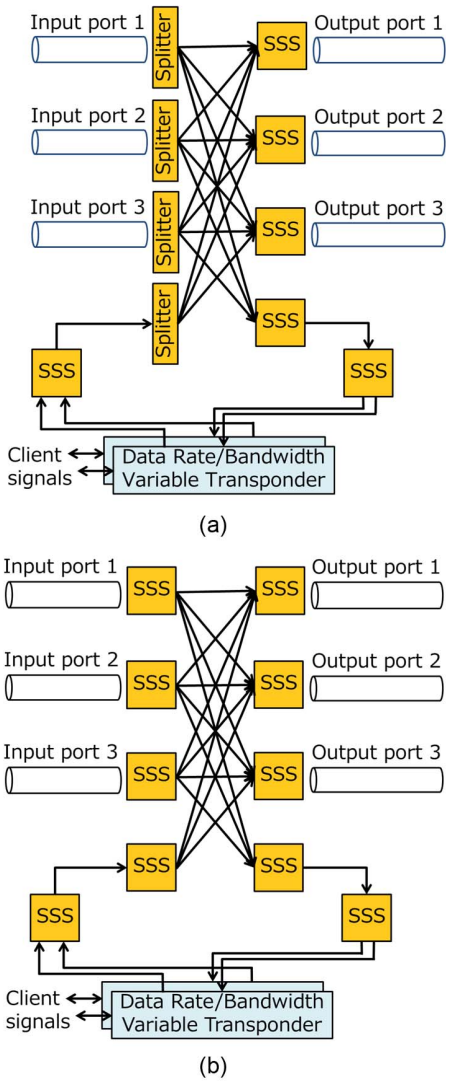

Fig. 3. Traditional optical node architectures for EONs. (a) Broadcast-and-select architecture. (b) Spectrum-routing architecture.

is usually implemented using large-port-count optical switches like a 3D-MEMS, which interconnects input/output ports and diverse building modules, such as the SSS, multiplexer (MUX), demultiplexer (DEMUX), EDFA, PLZT devices, and so on. These interconnections in the optical backplane are dynamically reconfigured according to the request for signal switching and/or processing. Moreover, it is easy to add extra functions (e.g., wavelength conversion) because the arrangement of these building modules is not fixed. Therefore, an AoD node has greater flexibility and upgradability than other static optical node architectures.

Multigranular transmission in the space/frequency/time domain has been demonstrated using AoD nodes and MCFs [14]. An experiment demonstrated the great flexibility of an AoD node in MCF-based EONs with over 6000-fold bandwidth granularity. Reference [15] defines the flexibility of node architectures on the basis of the entropy of the system and compares those of AoD nodes and traditional static node architectures of EONs. The advantage on the flexibility of AoD nodes has been proved both theoretically and experimentally. Reference [16] first demonstrated WDM inter-data center network (DCN) transmission using AoD nodes. In this model, clustered DCNs are connected through metro/core networks, and inter- and intracluster transmission is conducted according to the AoD concept.

Moreover, the flexibility of AoD nodes can also be used to reduce the power consumption of optical nodes. Because AoD nodes are dynamically constructed according to the switching request, they can use just enough modules, although traditional architectures constantly require a fixed maximum number of hard-wired modules regardless of the request. It is possible that the use of AoD nodes can reduce the number of implemented modules and the power consumption. References [17,18] include a power-consumption analysis for AoD nodes. Reference [17] shows that using AoD nodes can reduce the total power consumption of the network by more than 25% using a heuristic algorithm to construct AoD nodes. Reference [18] numerically analyzes the benchmark of power-consumption reduction according to the granularity of the switching request.

Despite these great advantages, AoD nodes also have some challenges. In this paper, the two important problems of AoD nodes are addressed. One is the scalability problem of the optical backplane. As shown in Fig. 1, all the building modules implemented in an AoD node are connected to a central optical backplane (3D-MEMS). When the number of input/output ports and building modules is increased, the port count required for the optical backplane is too large to be implemented by a single 3D-MEMS. Using multiple 3D-MEMSs is a simple solution to this problem; however, to switch signals between multiple 3D-MEMSs freely, many 3D-MEMSs ports are used for intraconnections between them. A sophisticated AoD construction using multiple 3D-MEMSs is required because wasting the switching ports of a 3D-MEMS requires more 3D-MEMSs and increases the power consumption of AoD nodes. The other problem is a trade-off between the switching granularity and the number of required modules. Although some studies have examined the energy efficiency of AoD nodes, reducing their power consumption depends on reducing the number of SSSs, assuming switching requests with coarse granularity, such as fiber switching. If EONs require fully flexible operation for all input/output ports of AoD nodes, they require the same number of SSSs as traditional architectures.

C. Routing and Spectrum Assignment Problem for AoD Nodes

The routing and spectrum assignment (RSA) problem is the most important problem concerning EONs from the perspective of networking [19,20]. Here, the unit of the assigned spectrum resource in EONs, the frequency slot (FS), is regarded as the wavelength in WDM networks. In optical networks, various network services are requested dynamically, and the network traffic changes greatly and rapidly with time. Therefore, it is important to use dynamic approaches to solve the RSA problem [21]. Reference [22]

compares dynamic spectrum allocation in three flexibility scenarios: fixed, semielastic, and elastic network scenarios. The RSA problem is equivalent to the routing and wavelength assignment (RWA) problem in traditional WDM networks. However, the RSA problem exhibits different characteristics owing to its flexible resource management. Spectrum fragmentation is one of the issues that must be challenged in the RSA problem but not the RWA problem. In EONs, the spectrum resources are fragmented by repeated dynamic setup and release of these heterogeneous bandwidth connections [23]. Reference [24] proposes two defragmentation algorithms using the path connectivity in flexible bandwidth networks. The path connectivity reveals the difficulty of transmitting traffic in the optical path on the basis of the spectral usage matrix. Reference [25] experimentally evaluates the proposed fragmentation-aware routing and spectrum allocation algorithms in a software-defined network enabled by OpenFlow. There are various studies of RSA problems aimed at improving other performance characteristics of EONs [26,27]. Reference [26] proposes a quality-of-transmission-aware RSA method by focusing on the optical signal-to-noise ratio metric of optical paths. Reference [27] tries to solve the power-consumption problem from the perspective of resource allocation. Reference [28], which is our previous work, reveals how the intercore cross talk of multicore fibers is reduced by a dynamic resource allocation method.

When AoD nodes are implemented for EONs, the RSA problem and resource allocation method become more serious concerns. AoD nodes dynamically construct themselves and supply the signal switching and/or processing according to the requests; therefore, the arrangement of allocated spectra (which is the result of resource allocation) affects the AoD node configurations [11]. Several studies have examined a dynamic resource allocation method considering the construction of AoD nodes [29,30]. Reference [29] numerically analyzes RSA solutions in MCF-based EONs that reduce intercore cross talk of MCFs considering AoD nodes. The proposed RSA strategy also reduces the number of SSSs and amplifiers in AoD nodes. Reference [30] proposes a redundant optical node configuration method based on AoD nodes for restoration from component failure. It also addresses a routing algorithm that improves the lightpath availability by increasing the fiber switching requests. However, these studies assume not a dynamic but a static model of performance evaluation. It is necessary to study a dynamic resource allocation method considering AoD node configuration. We have already studied the dynamic resource allocation considering the monetary cost of AoD nodes [31,32], but the proposed resource allocation methods and node architectures still have the problem of scalability and feasibility.

III. Energy-Efficient AoD Nodes

A. Concept

First, the concept of the proposed energy-efficient AoD node is introduced. Note that in this paper, although EONs are assumed to be equipped with MCFs, the proposed node architecture and resource allocation method can also be applied to an EON that has multiple single-core single-mode fibers in one link.

In the proposed energy-efficient AoD node architecture, a large proportion of the SSSs are replaced by an array-waveguide-grating-based MUX/DEMUX to reduce power consumption. A MUX/DEMUX is a fixed-grid-building module whose output/input ports and wavelength channels are in a one-to-one correspondence. Spectra with the same bandwidth need to be allocated in a transmission signal if it is processed by a MUX/DEMUX. Figure 4 shows the difference between traditional spectrum allocation and the proposed spectrum allocation considering energy-efficient AoD nodes. The proposed spectrum allocation method simplifies the building modules in the proposed energy-efficient AoD nodes. It is explained in detail in the next section.

Figure 4(a) shows the traditional nonuniform spectrum allocation in EONs. When MCFs are installed in EONs, each input or output port of the optical nodes is connected to a core of MCFs. Because of the repeated setup and release of connection having diverse bandwidth, the spectrum resources of EONs are fragmented; therefore, the efficiency of spectrum utilization is decreased. On the other hand, the proposed uniform spectrum allocation shown in Fig. 4(b) can reduce the spectrum fragmentation by classifying connections according to the required bandwidth. Moreover, in terms of the node architecture, this uniform spectrum allocation also makes it possible to replace flexible SSSs with fixed-grid MUX/DEMUXs according to the dynamic and adaptive construction of AoD nodes. In this paper, cores in which connections requiring the same

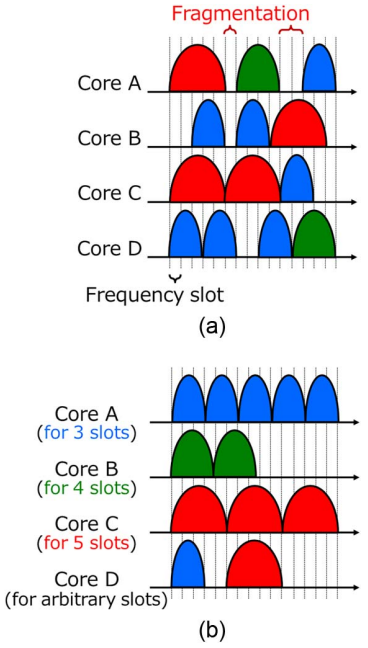

Fig. 4. (a) Traditional spectrum allocation. (b) Example of spectrum allocation considering energy-efficient AoD nodes.

bandwidth are allocated [such as core A, B, and C in Fig. 4(b)] are called *dedicated cores*, and cores in which connections requiring arbitrary bandwidth are allocated [such as core D in Fig. 4(b)] are called *common cores*. The common cores are preserved to accommodate the traffic, overflowed from fixed-grid dedicated cores, which leads to the flexibility of the traffic accommodation in the proposed node. The number of common cores and dedicated cores is statically established before network operation begins; however, the number of dedicated cores for the λ slots is set dynamically. First, a connection requiring an arbitrary number of FSs can be allocated to an empty dedicated core, which leads to the flexibility of the traffic accommodation in the proposed node. Once the connection is allocated to the empty dedicated core, subsequent connections requiring the same number of FSs must be allocated to that dedicated core.

B. Architecture of the Energy-Efficient AoD Nodes

The architecture of the proposed energy-efficient AoD nodes is shown in Fig. 5. Note that two dotted lines are the examples of optical switching, and they are explained in the next paragraph. Optical switching in these AoD nodes is divided into three phases, as shown in Fig. 5. This is because the number of required switching ports is too large to be constructed if the implementation depends on the single central optical backplane. The scalability issues based on the intraconnections of 3D-MEMSs in a single backplane are dramatically mitigated by the multistep switching scheme.

Signals are switched in this architecture as follows. First, input signals are switched to appropriate building modules in the core switching phase. If input signals are from common cores, then such signals having various spectral width are processed by an SSS in the wave band switching phase. In this part, spectra with the same width are grouped and switched to the corresponding DEMUXs. Note that the color of the MUX/DEMUXs in our figures represents the supported spectral width. On the other hand, if the input signals are from dedicated cores, then, skipping the wave band switching phase, such signals are directly switched to the corresponding DEMUXs in the wavelength switching phase. In the wavelength switching phase, switched input signals from dedicated cores and the corresponding wave band group from an SSS are demultiplexed into a wavelength channel in DEMUXs. Each wavelength channel is switched to the corresponding MUX, which is connected to an appropriate output port according to the switching request.

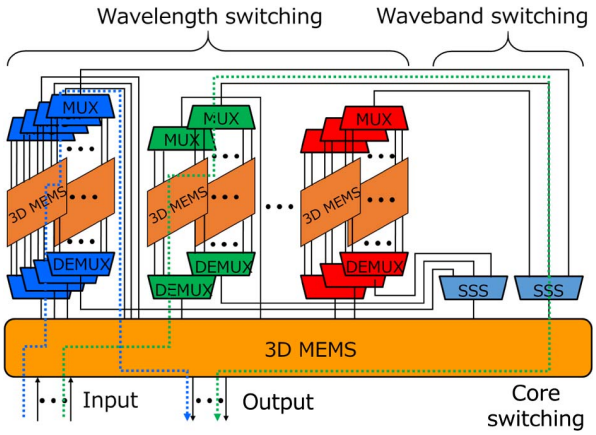

Fig. 5. Proposed AoD node architecture.

Figure 5 also shows examples of signal switching and processing. The blue dotted line represents a connection requiring three FSs, and its switching request is from a dedicated core to a dedicated core. The input signal in a dedicated core for three FSs is first demultiplexed by a blue DEMUX (which is for three FSs) after the core switching phase, then delivered to a blue MUX through the wavelength switching phase. The signal is finally delivered to the output dedicated core, which is for three FSs. The green dotted line represents a connection requiring four FSs, and its switching request is from a dedicated core to a common core. The input signal in a dedicated core for four FSs is first demultiplexed by a green DEMUX (which is for four FSs) after the core switching phase, then delivered to a green MUX through the wavelength switching phase. Next, the signal is delivered to an SSS through the wave band switching phase. In this SSS, the signal is combined with other signals that have different spectral width and finally delivered to the output common core.

The proposed architecture in Fig. 5 has the same number of input/output ports; however, this architecture also supports the case when the numbers of input/output ports are different. In such a case, the scale of the 3D-MEMSs, which are used for wavelength switching, depends on the higher port count.

C. Numerical Analysis and Static Evaluation

In this subsection, the proposed energy-efficient AoD nodes are numerically analyzed, with a focus on the required number of building modules and power consumption. The symbols used in this section are summarized in Table I. Note that the number of DEMUXs is the same as that of MUXs, and this number is determined in advance

TABLE I
SYMBOLS USED IN THE NUMERICAL ANALYSIS OF THE PROPOSED ARCHITECTURE

Symbols	Description
F	Number of FSs per core
P	Port count of AoD nodes (supporting $P \times P$ switching)
C	Number of cores of a single installed MCF
$\Delta\lambda$	Channel spacing (number of FSs)
$N^{\Delta\lambda}_{\mathrm{MUX}}$	Number of implemented $\Delta\lambda$-MUXs
P_{MEMS}	Port count of 3D-MEMSs (supporting $P_{\mathrm{MEMS}} \times P_{\mathrm{MEMS}}$ switching)
W_{MEMS}	Power consumption of a 3D-MEMS
W_{SSS}	Power consumption of an SSS
W_{AoD}	Total power consumption of the proposed AoD node

according to the number of all types of dedicated cores that are connected to the AoD node to maintain full flexibility in the spectral width setup for dedicated cores. In this paper, for simplicity, the power consumption of an optical node is defined as the sum of the power consumption of all SSSs and 3D-MEMSs in operation.

The number of ports of a MUX/DEMUX whose channel spacing (width of the spectral resolution) is $\Delta\lambda$ FSs is

$$P_{\mathrm{MUX}}^{\Delta\lambda} = \left\lfloor \frac{F}{\Delta\lambda} \right\rfloor. \tag{1}$$

The value $P_{\mathrm{MUX}}^{\Delta\lambda}$ also represents the number of wavelength channels per core. Then, for wavelength switching of $\Delta\lambda$ FSs, the number of ports of the 3D-MEMS per corresponding $\Delta\lambda$-MUX is

$$\mathrm{Ch}_{\mathrm{MEMS}}^{\Delta\lambda} = \left\lfloor \frac{P_{\mathrm{MEMS}}}{N_{\mathrm{MUX}}^{\Delta\lambda}} \right\rfloor. \tag{2}$$

It is equal to the maximum number of wavelength channels that are switched in one 3D-MEMS because the same port from each $\Delta\lambda$-MUX/DEMUX has to be connected to the same 3D-MEMS to switch the corresponding wavelength channel. The number of 3D-MEMSs used for wavelength switching with a channel spacing of $\Delta\lambda$ FSs is

$$N_{\mathrm{MEMS}}^{\Delta\lambda} = \left\lceil \frac{P_{\mathrm{MUX}}^{\Delta\lambda}}{Ch_{\mathrm{MEMS}}^{\Delta\lambda}} \right\rceil = \left\lceil \frac{\left\lfloor \frac{F}{\Delta\lambda} \right\rfloor}{\left\lfloor \frac{P_{\mathrm{MEMS}}}{N_{\mathrm{MUX}}^{\Delta\lambda}} \right\rfloor} \right\rceil. \tag{3}$$

Therefore, the total number of 3D-MEMS required in the proposed AoD node is

$$N_{\mathrm{MEMS}} = 1 + \sum_{\Delta\lambda} \left\lceil \frac{\left\lfloor \frac{F}{\Delta\lambda} \right\rfloor}{\left\lfloor \frac{P_{\mathrm{MEMS}}}{N_{\mathrm{MUX}}^{\Delta\lambda}} \right\rfloor} \right\rceil. \tag{4}$$

Because the number of MUXs is less than the number of input/output ports of an optical node ($N_{\mathrm{MUX}}^{\Delta\lambda} \le P$),

$$N_{\mathrm{MEMS}} \le 1 + \sum_{\Delta\lambda} \left\lceil \frac{\left\lfloor \frac{F}{\Delta\lambda} \right\rfloor}{\left\lfloor \frac{P_{\mathrm{MEMS}}}{P} \right\rfloor} \right\rceil. \tag{5}$$

Next, the number of SSSs required in the proposed AoD node N_{SSS} is the same as the number of common cores N_{COM}. The number of common cores is statically determined in advance, and one common core is set up for every C cores. The value is determined from preliminary simulation results. When all the input/output ports are connected to the cores of the MCFs,

$$N_{\mathrm{SSS}} = N_{\mathrm{COM}} = \left\lceil \frac{P}{C} \right\rceil. \tag{6}$$

Therefore, the total power consumption of the proposed AoD node is

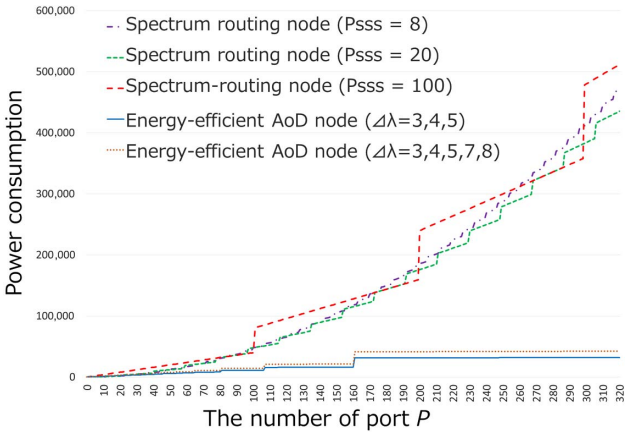

Fig. 6. Static evaluation of power consumption for EONs.

$$W_{\mathrm{AoD}} = W_{\mathrm{SSS}} \cdot N_{\mathrm{SSS}} + W_{\mathrm{MEMS}} \cdot N_{\mathrm{MEMS}} \le W_{\mathrm{SSS}} \cdot \left\lceil \frac{P}{C} \right\rceil + W_{\mathrm{MEMS}} \cdot \left(1 + \sum_{\Delta\lambda} \left\lceil \frac{\left\lfloor \frac{F}{\Delta\lambda} \right\rfloor}{\left\lfloor \frac{P_{\mathrm{MEMS}}}{P} \right\rfloor} \right\rceil \right). \tag{7}$$

Figure 6 shows the numerically analyzed total power consumption of EONs. In this figure, the vertical axis represents the total power consumption of each node, and the horizontal axis represents the port count of each node.

The evaluation is based on Eqs. (7) and (A3) described in Appendix A. Static values are defined as follows. The number of spectrum slots F is 320, because we set the width of the FS to 12.5 GHz and the total spectrum resource per core to 4 THz (C band). The port count of a single SSS P_{SSS} is 20. The port count of a single 3D-MEMS P_{MEMS} is 320. The power-consumption values W_{SSS} and W_{MEMS} are 40 and 150, respectively. Figure 6 shows an explosive increase in the power consumption of the traditional spectrum-routing node architecture [shown in Fig. 3(b)] with port count growth. In this analysis, there are three spectrum-routing nodes that are different in the number of ports supported by a single SSS P_{SSS}: 8, 20, and 100. Note that the power consumption of SSS is assumed to be directly proportional to the number of ports. Use of the proposed energy-efficient AoD node can dramatically mitigate the increase, although the larger number of types of required spectral width slightly increases the node's power consumption.

IV. On-Demand Routing and Spectrum Allocation for Energy-Efficient AoD Nodes

A. Concept and Definition of Allocation Cost

In this section, the procedure for the proposed on-demand routing and spectrum allocation method is explained in detail. The proposed allocation method is controlled according to the *allocation cost* of spectra. The allocation cost is defined for each spectrum of all the MCFs according to the status of a core to lower the allocation cost

of a desirable spectrum. There are three types of allocation costs for a combination of a route and spectrum (k,f), where the selected route is k, and the initial FS of the selected spectrum is f. These three types of allocation costs are defined as follows. The symbols used in the proposed routing and allocation method are summarized in Table II.

$X_{l,c}^{k,f}$ is the most basic allocation cost and represents the allocation costs of a core c ($c \in \mathcal{C}_l, l \in \mathcal{L}_k$) for (k,f). When the required number of spectrum slots is r,

$$X_{l,c}^{k,f} = \begin{cases} 1-u_c & \text{if } c \text{ is a core for } r \text{ slots,} \\ 1 & \text{if } c \text{ is an empty dedicated core,} \\ H_k+1 & \text{if } c \text{ is a common core.} \end{cases} \quad (8)$$

Otherwise, the cost $X_{l,c}^{k,f} = \infty$ (i.e., the selected spectrum is occupied and cannot be allocated). In our proposed method, the desirable core is the dedicated core for r slots from the perspective of spectrum fragmentation. Moreover, the dedicated core for r slots with the lowest spectrum utilization is the most desirable to maintain a large number of empty dedicated cores.

$X_l^{k,f}$ is the intermediate allocation cost, which represents the allocation costs of a link l ($l \in \mathcal{L}_k$) for (k,f):

$$X_l^{k,f} = \min\{X_{l,c}^{k,f} | c \in \mathcal{C}_l\}. \quad (9)$$

This allocation cost is the cost of a desirable core in link l.

$X^{k,f}$ is the final allocation cost, which represents the allocation costs for (k,f). Its value is the sum of $X_l^{k,f}$ at each link along the route k. Therefore, $X^{k,f}$ is calculated as follows:

$$X^{k,f} = \sum_{l \in \mathcal{R}_k} X_l^{k,f}. \quad (10)$$

All these costs are updated when an optical path is set up or released because the actual value of each cost depends only on the state of spectrum utilization, meaning that after connection arrival, the spectrum allocation process does not calculate but refers the appropriate cost to reduce the processing delay.

TABLE II
SYMBOLS USED IN THE PROPOSED SPECTRUM AND CORE ALLOCATION

Symbols	Description
f	Index of an initial FS
l	Index of a link
c	Index of a core
k	Index of a route that is one of the precalculated routes
H_k	Number of hops of route k
$\mathcal{L}_k$	Set of links in route k
$\mathcal{C}_l$	Set of cores at link l
u_c	Spectrum utilization of core c

B. Flow Chart and Example of Allocation-Cost Calculation

Figure 7 shows the optical path-provisioning flow chart of the proposed routing and spectrum allocation method. When a new connection request arrives, the number of required FSs is calculated for each route k. Next, $X^{k,f}$ is calculated for each (k,f). If the minimum allocation cost $X^{k,f}$ is ∞, there is no available combination of a route and spectrum resources, and the connection request is rejected. Otherwise, the route and spectrum (k,f) are selected to minimize $X^{k,f}$. Then, the selected spectrum is allocated to the core c with a minimum $X_{l,c}^{k,f}$ for each link along the route k. Finally, all the $X_{l,c}^{k,f}$ values are updated according to the changed status of the cores, and path provisioning succeeds.

Figure 8 shows an example of a cost calculation when the number of required FSs is three and the index of the initial FS is one. The selected route ($k = 2$) from node A to node D has three links ($l = 1, 2$, and 3). Hence, $H_2 + 1$ is equal to 4.

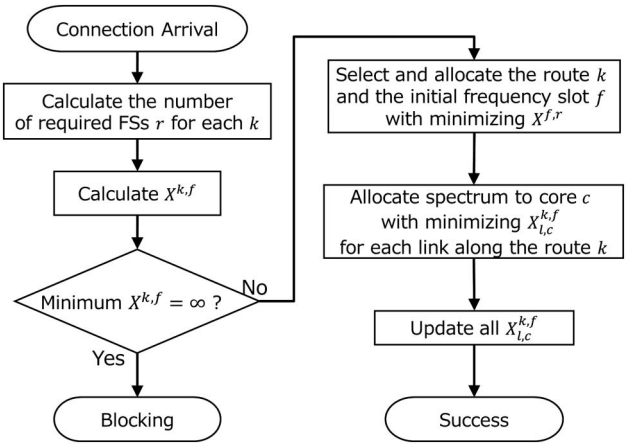

Fig. 7. Flow chart of the proposed routing and spectrum allocation method.

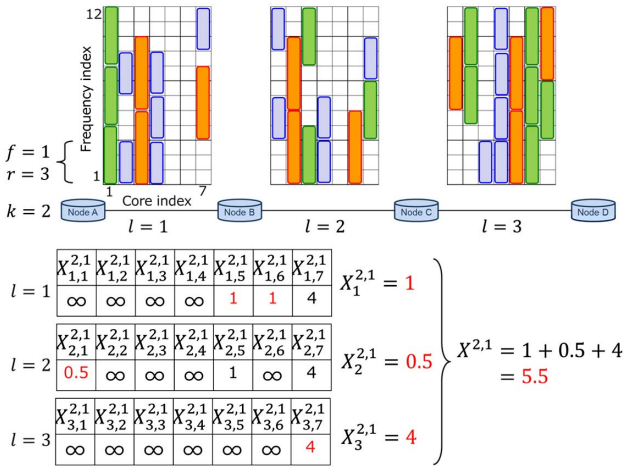

Fig. 8. Example of an allocation cost calculation.

At each link, the minimum value of $X_{l,c}^{2,1}$ is selected as the $X_l^{2,1}$ value ($X_1^{2,1}=1, X_2^{2,1}=0.5$, and $X_3^{2,1}=4$). The cost of spectrum $X^{2,1}$ is the sum of these $X_l^{2,1}$ values ($X^{2,1}=X_1^{2,1}+X_2^{2,1}+X_3^{2,1}=5.5$).

V. Performance Evaluation

A. Simulation Model

We used our own C++ simulator to evaluate the proposed method. We adopted the JPN-12 topology, USA topology, NSF topology, and Deutsche Telekom (DT) topology shown in Figs. 9–12, respectively. The JPN-12 topology has 12 nodes and 16 links. The USA topology has 28 nodes and 45 links. The NSF topology has 14 nodes and 21 links. The DT topology has 14 nodes and 23 links. Each link has three MCFs for each direction. We simply suppose that all MCFs have seven cores. We set the width of the FS to 12.5 GHz and the total spectrum resource per core to 4 THz (C band). Therefore, the number of FSs per core is $W=320$. We assume that the service time and the interarrival time of the connection requests follow an exponential distribution. Connections require 40, 100, or 400 Gbps transmission randomly. The number of required FSs depends on the bitrate and the hop count of the selected route. Table III shows the required FS setup for the adopted topology scaled from the setup in Ref. [33]. Note that "short," "intermediate," and "long" are defined as follows when M is the maximum number of hops of all candidate routes:

- short: $0 < h \le \left\lceil \frac{M}{3} \right\rceil$,
- intermediate: $\left\lceil \frac{M}{3} \right\rceil < h \le \left\lceil 2 \cdot \frac{M}{3} \right\rceil$,
- long: $\left\lceil 2 \cdot \frac{M}{3} \right\rceil < h \le M$.

The traffic load is definite for all source–destination pairs. Further, $k=5$ in the k-shortest path algorithm. The number of common cores is one for each MCF. The parameters of the building modules are shown in Table IV [34]. Note that the 3D-MEMS and SSS can be turned off when they are not in use. We introduce spectrum routing (SR) with first fit of the FS index (FFS) and SR with first fit of the core index (FFC) as comparison methods. Both of these methods suppose that SR node architecture [15] is implemented for EONs. From the k-shortest paths ($k=5$), both comparison methods select one route that has the least congested bottleneck link. SR with FFS allocates spectra for the FFS. SR with FFC allocates spectra for

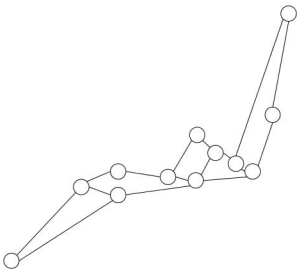

Fig. 9. JPN-12 topology.

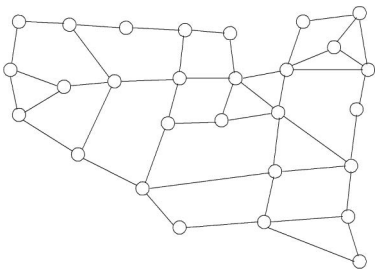

Fig. 10. USA topology.

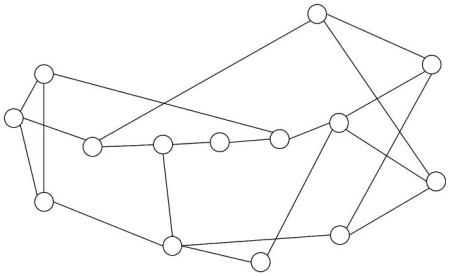

Fig. 11. NSF topology.

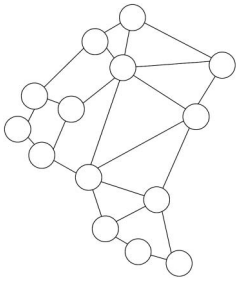

Fig. 12. DT topology.

TABLE III
Number of Required FSs

# of Hops	# of Required FSs		
	40 Gbps	100 Gbps	400 Gbps
Short	3	3	7
Intermediate	3	4	7
Long	4	5	8

TABLE IV
Parameters of 3D-MEMS and Building Modules

Module	Port Count	Power Consumption [W]
MUX/DEMUX	$\lfloor 320/\Delta\lambda \rfloor$	0
SSS	20	40
3D-MEMS	360	150

the FFC. The combination of proposed energy-efficient node and resource assignment is denoted "Proposed system" in the evaluations.

B. Evaluations of Power Consumption

Figures 13–16 show the total power consumption of optical switching nodes. These figures show that the total power consumption is reduced by 50% at most by utilizing the proposed energy-efficient AoD nodes and cost-aware on-demand routing and spectrum allocation method. By comparing the proposed method with the better comparison method SR with FFC, the power-consumption reduction is high when the traffic load is high, and as the traffic load becomes low, the difference in power consumption becomes small. However, the superiority of the proposed method is lost only under extremely low traffic load conditions in which all connection requests are not blocked, as shown by evaluations of the blocking probability in the next subsection. As a result, the proposed energy-efficient AoD node and resource allocation method can usually reduce the power consumption of optical switching nodes in dynamically operated EONs by arrangement of spectra and simplification of required building modules.

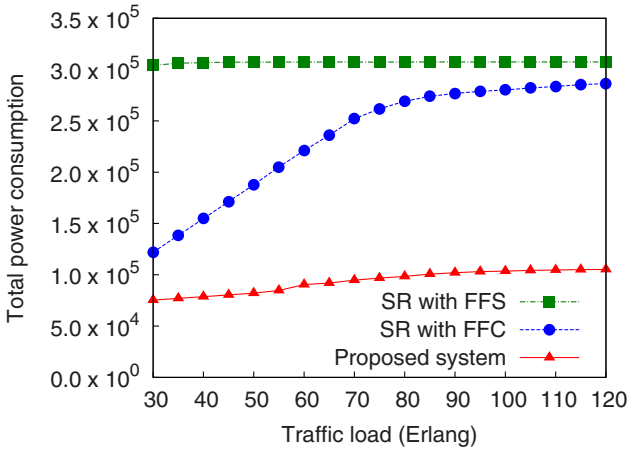

Fig. 13. Total power consumption (JPN-12).

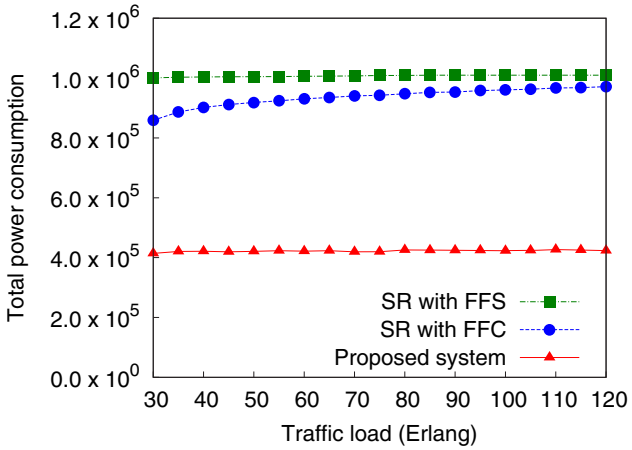

Fig. 14. Total power consumption (USA).

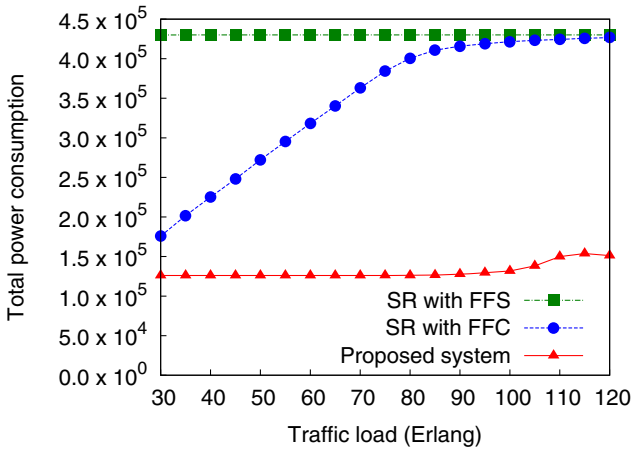

Fig. 15. Total power consumption (NSF).

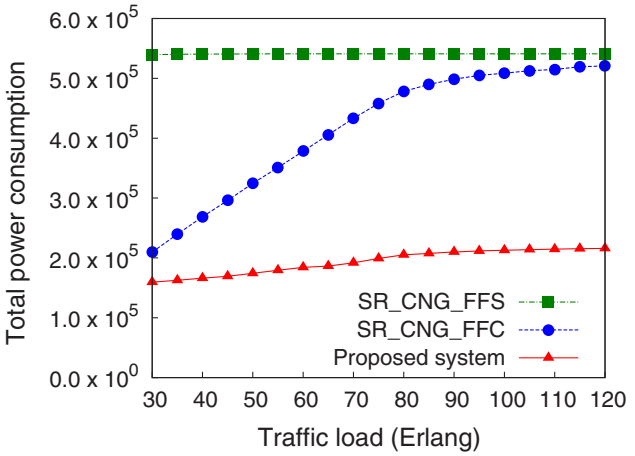

Fig. 16. Total power consumption (DT).

C. Evaluations of Blocking Probability

Figures 17–20 show the blocking probability of the entire network. These figures show that the blocking probability performance of the proposed method outperforms that of the comparison methods except in the USA topology. In the USA topology, the blocking probabilities are almost the same among all the methods. Therefore, the proposed resource allocation method reduces the power consumption without degrading the blocking probability.

In terms of the dependence of the blocking probability on the topology, the performance of the proposed method is relatively poor for the topology in which the blocking probability is high at low erlang. This means that these topologies have many k-shortest paths that include a few of the same links (these links are particularly congested and obviously bottleneck links) because the traffic volume

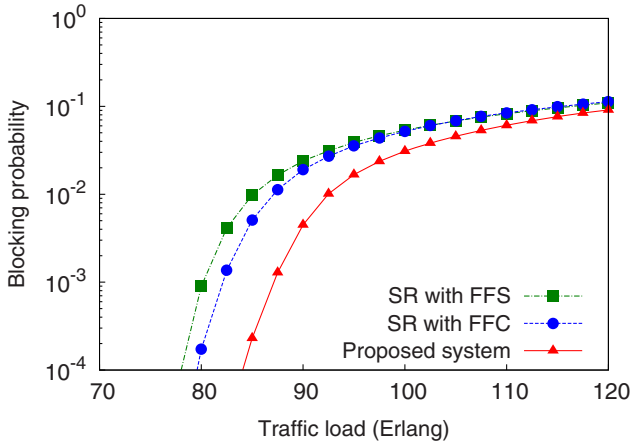

Fig. 17. Blocking probability (JPN-12).

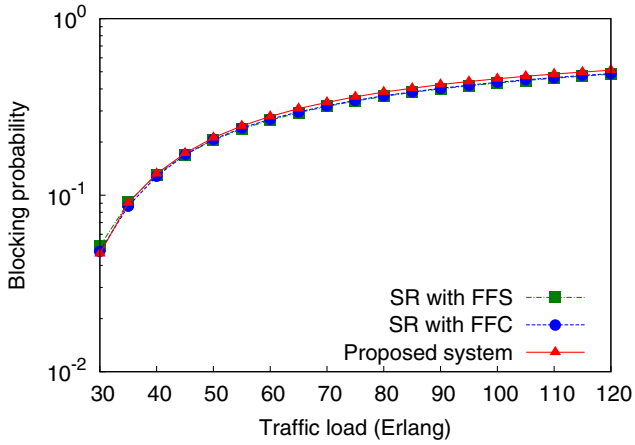

Fig. 18. Blocking probability (USA).

for each source–destination pair has the same value in these evaluations. This characteristic is analyzed as follows, with a focus on "betweenness centrality" and "betweenness centralization," which are feature values of a topology.

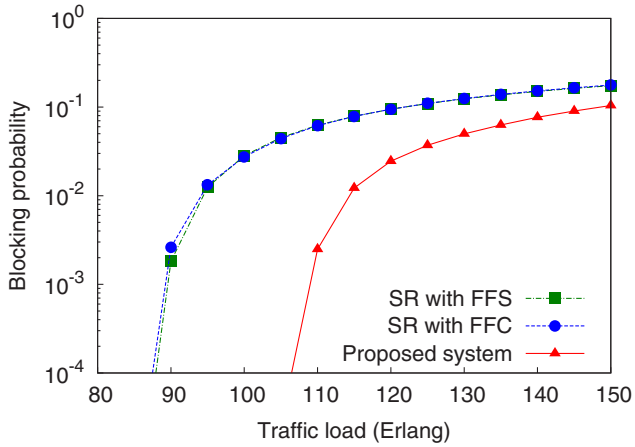

Fig. 19. Blocking probability (NSF).

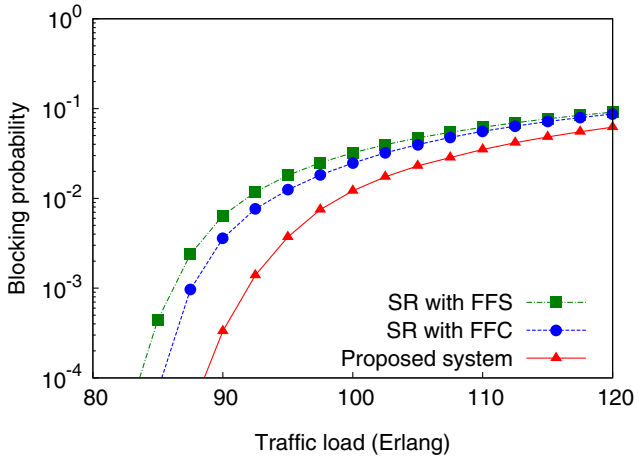

Fig. 20. Blocking probability (DT).

When the number of nodes is V, node betweenness centrality for node v_i is defined as

$$C_B(v_i) = \frac{\sum_{s;s\neq i}^{V}\sum_{t;t\neq i,s}^{V}\frac{g_i(v_s,v_t)}{N_{v_s,v_t}}}{\frac{(V-1)(V-2)}{2}}. \tag{11}$$

Note that $g_i(v_s, v_t)$ is the number of shortest paths from v_s to v_t through v_i, and N_{v_s,v_t} is the total number of shortest paths from v_s to v_t.

According to the definition of node betweenness centrality, the link betweenness centrality for link l_i is newly defined as

$$C_B(l_i) = \frac{\sum_{s}^{V}\sum_{t;t\neq s}^{V}\frac{g_i'(v_s,v_t)}{N_{v_s,v_t}}}{V\cdot(V-1)}. \tag{12}$$

Note that $g_i'(v_s, v_t)$ is the number of shortest paths from v_s to v_t through l_i.

Betweenness centralization is a feature value that becomes small when the betweenness centralities of a few links or nodes are particularly high. On the basis of the link betweenness centrality, the link betweenness centralization is defined as

$$\frac{\max_i\{C_B(l_i)\}}{\sum_j\{\max_i\{C_B(l_i)\} - C_B(l_j)\}}. \tag{13}$$

Table V shows the link betweenness centralizations of all the topologies that are adopted in the evaluations. From Table V and Figs. 17–20, as the performance of the

TABLE V
LINK BETWEENNESS CENTRALIZATIONS

Topology	Link Betweenness Centralizations
JPN	0.0599⋯
USA	0.0171⋯
NSF	0.0603⋯
DT	0.0422⋯

proposed method improves, the link betweenness centralizations increase. Therefore, both the blocking probability and power consumption can be improved dramatically by designing a topology so that its link betweenness centralization becomes high because a reduction of power consumption is not dependent on an adopted topology (as shown in Figs. 13–16). According to the definition, high link betweenness centralization means each link betweenness centrality tends to take a value close to the maximum value. When many links have high link betweenness centrality, these links tend to be congested similarly on the basis of Eq. (12). This means that a topology with high link betweenness centralizations does not have a specific bottleneck link, and the traffic load of each link is more uniform in such a topology. Therefore, the proposed method is suited for the actual network topology, in which it is desired that the traffic load of each link is as uniform as possible.

D. Evaluations of Scalability

Figures 21–24 show the scalability of power consumption of optical switching nodes. The vertical axis indicates total power consumption (same as in Subsection V.B), and the horizontal axis indicates the number of cores per link. The values of the traffic load are 90, 30, 115, and 100 in Figs. 21–24, respectively. These figures show that the power consumption of the proposed method is less than that of the compared methods, and the difference becomes large as the number of cores becomes large. Although MCFs that have more than 30 cores have already been presented, the tendency of these evaluations is clear when the number of cores per link is under 30. Moreover, the shapes of these four figures are similar to that of numerically analyzed Fig. 6. Therefore, the proposed method is suited for the future large optical nodes, and it represents superior scalability of power consumption.

Figures 25–28 show the scalability of the blocking probability of the entire network. The vertical axis indicates the blocking probability of path setup requests (the same as in Subsection V.C), and the horizontal axis indicates the

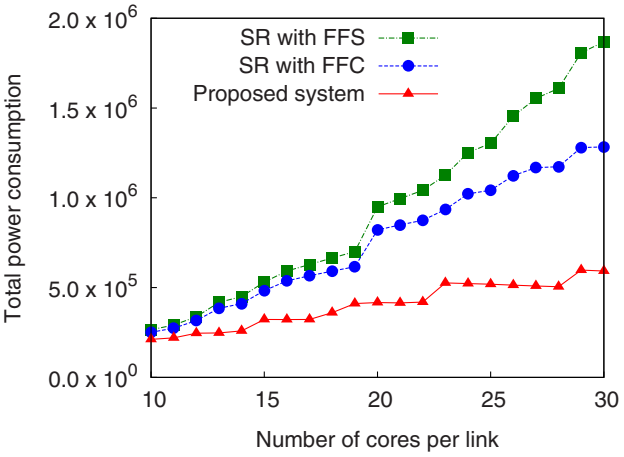

Fig. 22. Scalability of power consumption (USA).

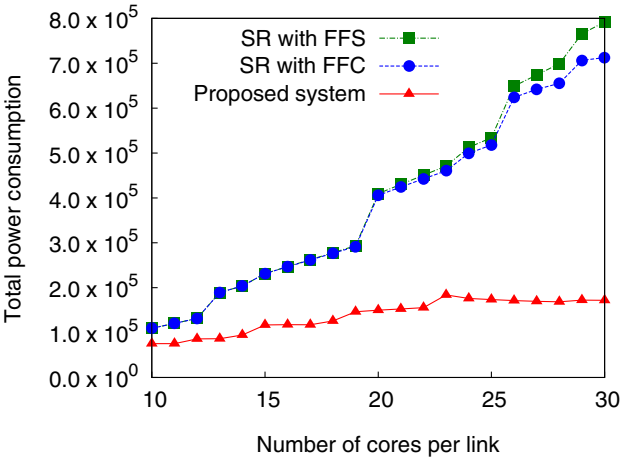

Fig. 23. Scalability of power consumption (NSF).

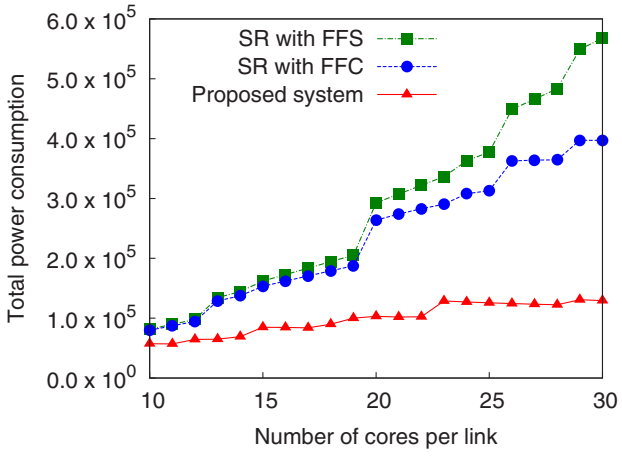

Fig. 21. Scalability of power consumption (JPN-12).

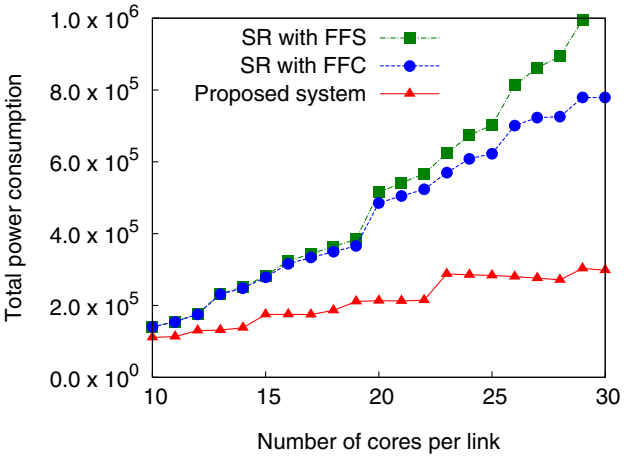

Fig. 24. Scalability of power consumption (DT).

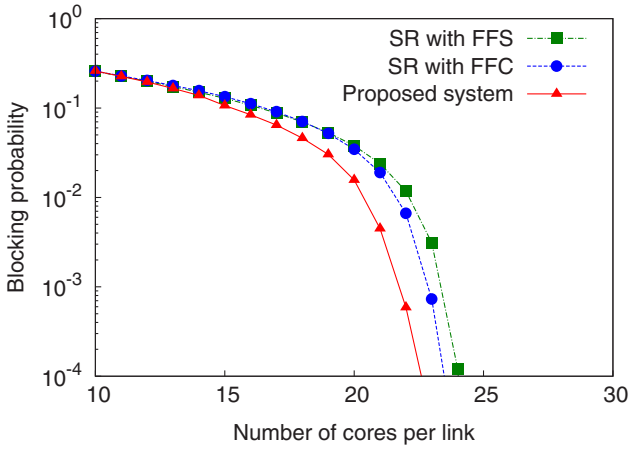

Fig. 25. Scalability of blocking probability (JPN-12).

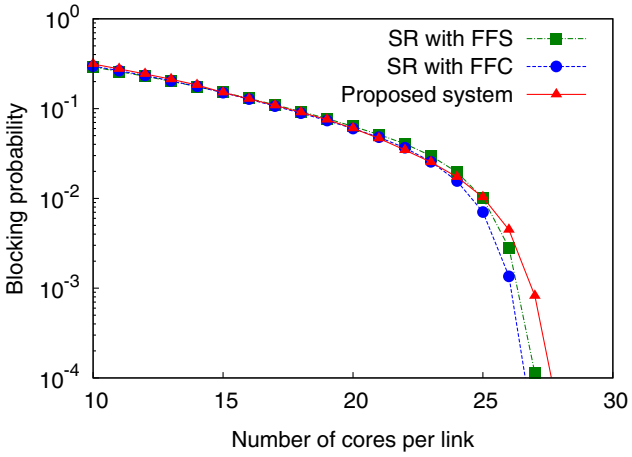

Fig. 26. Scalability of blocking probability (USA).

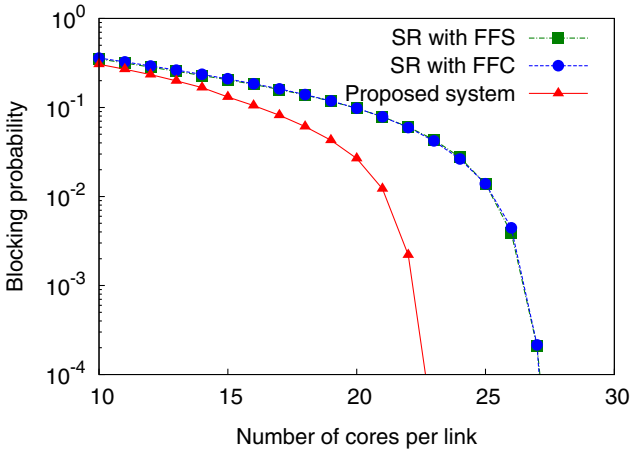

Fig. 27. Scalability of blocking probability (NSF).

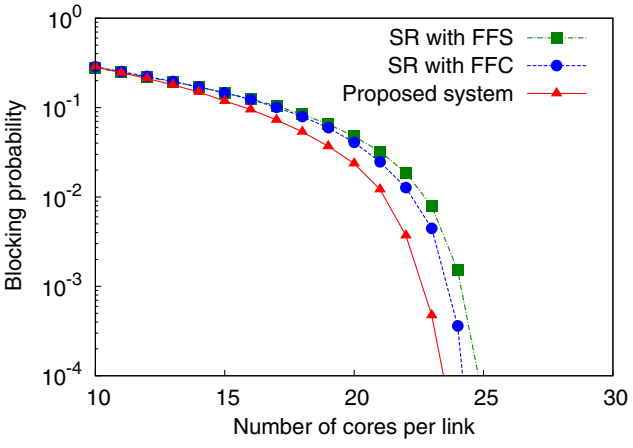

Fig. 28. Scalability of blocking probability (DT).

number of cores per link. The values of traffic load are 80, 30, 105, and 90 in Figs. 25–28, respectively. These figures show that the blocking probability of the proposed method becomes much lower than that of the two compared methods as the number of cores becomes large in all topologies except USA topology. This is because there is more flexibility in the setup of dedicated cores for the proposed method when the number of cores is larger, and that effectively reduces the blocking probability. On the other hand, in the USA topology, the blocking probability of the proposed method is worse than that of the two compared methods. This is because a topology with a low link betweenness centralization, which is like the USA topology, has a specific bottleneck link, and many connections are affected by the congested bottleneck. In this case, the reduction of degrees of freedom due to the dedicated cores is more serious than spectral defragmentation by dedicated cores. Therefore, in such a topology, the performance of the blocking topology may be inferior to the compared methods. However, it is possible to solve the problem of blocking probability by focusing on the scenario of actual network topologies (as mentioned in Subsection V.C).

VI. Conclusions

An EON with MCFs is expected to exhibit greater transmission capacity. In terms of energy efficiency, however, the power consumption of a traditional optical node is expected to increase explosively because of the port-count characteristics of SSSs. In this paper, we proposed an energy-efficient optical network system. We first discussed the proposed energy-efficient optical node architecture based on the AoD concept. Our proposed energy-efficient AoD node can reduce its power consumption by using fixed building modules containing MUX/DEMUXs. We also proposed a cost-aware resource allocation method that meets the requirements of the proposed node architecture. We evaluated the proposed method using extensive computer simulations. The proposed method can reduce the power consumption of optical nodes without degrading the blocking probability. Moreover, we showed that the proposed method can dramatically improve both the power

consumption and blocking probability if the network topology is appropriately designed, considering an index of link betweenness centralization.

In future work, it may be worthwhile to evaluate our proposed method for various other traffic models. Furthermore, other components of optical switching nodes that consume power, in addition to the switching and (de)multiplexing components, should be discussed.

Appendix A: Number of SSSs Required for Spectrum-Routing Node

It is supposed that spectrum-routing node supports $P \times P$ switching and each SSS supports $1 \times P_{\mathrm{SSS}}$ multiplexing/demultiplexing. If one SSS block in Fig. 3 needs to supply multiplexing/demultiplexing with more than P_{SSS} ports, the block is implemented by cascaded multiple SSSs. It is defined that cascaded N_{Cas} SSSs supply a $1 \times P_{\mathrm{Cas}}$ multiplexing/demultiplexing. When the SSS block is implemented by two-step cascaded SSSs ($1 \le N_{\mathrm{Cas}} \le P_{\mathrm{SSS}} + 1$),

$$P_{\mathrm{Cas}} = (N_{\mathrm{Cas}} - 1) \times P_{\mathrm{SSS}} + P_{\mathrm{SSS}} - (N_{\mathrm{Cas}} - 1). \tag{A1}$$

Because $P \le P_{\mathrm{Cas}}$,

$$\begin{aligned} P &\le (N_{\mathrm{Cas}} - 1) \times P_{\mathrm{SSS}} + P_{\mathrm{SSS}} - (N_{\mathrm{Cas}} - 1) \\ &= N_{\mathrm{Cas}} \cdot (P_{\mathrm{SSS}} - 1) + 1, \\ N_{\mathrm{Cas}} &\ge \frac{P-1}{P_{\mathrm{SSS}} - 1}, \\ N_{\mathrm{Cas}} &= \left\lceil \frac{P-1}{P_{\mathrm{SSS}} - 1} \right\rceil. \end{aligned} \tag{A2}$$

Therefore, the total number of SSSs required in spectrum-routing node N_{SR} is calculated as follows:

$$N_{\mathrm{SR}} = 2 \times P \times N_{\mathrm{Cas}} = 2 \cdot P \cdot \left\lceil \frac{P-1}{P_{\mathrm{SSS}} - 1} \right\rceil. \tag{A3}$$

Acknowledgment

This research was partly supported by the National Institute of Information and Communications Technology, Japan.

References

[1] M. Jinno, H. Takara, B. Kozicki, Y. Tsukishima, Y. Sone, and S. Matsuoka, "Spectrum-efficient and scalable elastic optical path network: Architecture, benefits, and enabling technologies," *IEEE Commun. Mag.*, vol. 47, no. 11, pp. 66–73, Nov. 2009.

[2] O. Gerstel, M. Jinno, A. Lord, and S. J. B. Yoo, "Elastic optical networking: A new dawn for the optical layer?" *IEEE Commun. Mag.*, vol. 50, no. 2, pp. s12–s20, Feb. 2012.

[3] A. Lord, P. Wright, and A. Mitra, "Core networks in the flexgrid era," *J. Lightwave Technol.*, vol. 33, no. 5, pp. 1126–1135, Mar. 2015.

[4] T. Morioka, "New generation optical infrastructure technologies: "EXAT initiative" towards 2020 and beyond," in *Opto Electronics and Communications Conf. (OECC)*, July 2009.

[5] S. Matsuo, K. Takenaga, Y. Sasaki, Y. Amma, S. Saito, K. Saitoh, T. Matsui, K. Nakajima, T. Mizuno, H. Takara, Y. Miyamoto, and T. Morioka, "High-spatial-multiplicity multicore fibers for future dense space-division-multiplexing systems," *J. Lightwave Technol.*, vol. 34, no. 6, pp. 1464–1475, Dec. 2016.

[6] T. Hayashi, Y. Tamura, T. Hasegawa, and T. Taru, "125-μm-cladding coupled multi-core fiber with ultra-low loss of 0.158 dB/km and record-low spatial mode dispersion of 6.1 ps/km1/2," in *Optical Fiber Communication Conf. (OFC)*, Mar. 2016, paper Th5A.1.

[7] B. Kozicki, H. Takara, Y. Tsukishima, T. Yoshimatsu, K. Yonenaga, and M. Jinno, "Experimental demonstration of spectrum-sliced elastic optical path network (SLICE)," *Opt. Express*, vol. 18, no. 21, pp. 22105–22118, Oct. 2010.

[8] B. Collings, "The next generation of ROADM devices for evolving network applications," in *Market Focus at European Conf. Optical Communication (ECOC) Exhibition*, Sept. 2011.

[9] B. Collings, "New devices enabling software-defined optical networks," *IEEE Commun. Mag.*, vol. 51, no. 3, pp. 66–71, Mar. 2013.

[10] H. Ishida, H. Hasegawa, and K. Sato, "Hardware scale and performance evaluation of a compact subsystem modular optical cross connect that adopts tailored add/drop architecture," *J. Opt. Commun. Netw.*, vol. 7, no. 6, pp. 586–596, June 2015.

[11] M. Garrich, N. Amaya, G. S. Zervas, P. Giaccone, and D. Simeonidou, "Architecture on demand: Synthesis and scalability," in *Conf. Optical Network Design and Modeling (ONDM)*, Apr. 2012.

[12] R. Younce, J. Larikova, and Y. Wang, "Engineering 400G for colorless-directionless-contentionless architecture in metro/regional networks," *J. Opt. Commun. Netw.*, vol. 5, no. 10, pp. A267–A273, Oct. 2013.

[13] A. Morea, J. Renaudier, T. Zami, A. Ghazisaeidi, and O. Bertran-Pardo, "Throughput comparison between 50-GHz and 37.5-GHz grid transparent networks," *J. Opt. Commun. Netw.*, vol. 7, no. 2, pp. A293–A300, Feb. 2015.

[14] N. Amaya, M. Irfan, G. Zervas, R. Nejabati, D. Simeonidou, J. Sakaguchi, W. Klaus, B. J. Puttnam, T. Miyazawa, Y. Awaji, N. Wada, and I. Henning, "Fully-elastic multi-granular network with space/frequency/time switching using multi-core fibres and programmable optical nodes," *Opt. Express*, vol. 21, no. 7, pp. 8865–8872, Apr. 2013.

[15] N. Amaya, G. Zervas, and D. Simeodinou, "Introducing node architecture flexibility for elastic optical networks," *J. Opt. Commun. Netw.*, vol. 5, no. 6, pp. 593–608, June 2013.

[16] S. Yan, E. Hugues-Salas, V. J. F. Rancano, Y. Shu, G. Saridis, B. R. Rofoee, Y. Yan, A. Peters, S. Jain, T. C. May-Smith, P. Petropoulos, D. J. Richardson, G. Zervas, and D. Simeonidou, "First demonstration of all-optical programmable SDM/TDM intra data centre and WDM inter-DCN communication," in *European Conf. Optical Communication (ECOC)*, Sept. 2014.

[17] A. Muhammad, G. Zervas, N. Amaya, D. Simeonidou, and R. Forchheimer, "Introducing flexible and synthetic optical networking: Planning and operation based on network function programmable ROADMs," *J. Opt. Commun. Netw.*, vol. 6, no. 7, pp. 635–648, July 2014.

[18] M. Garrich, N. Amaya, G. S. Zervas, J. R. F. Oliveira, P. Giaccone, A. Bianco, D. Simeonidou, and J. C. R. F. Oliveira,

"Architecture on demand design for high-capacity optical SDM/TDM/FDM switching," *J. Opt. Commun. Netw.*, vol. 7, no. 1, pp. 21–35, Jan. 2015.

[19] K. Christodoulopoulos, I. Tomkos, and E. A. Varvarigos, "Routing and spectrum allocation in OFDM-based optical networks with elastic bandwidth allocation," in *Global Telecommunications Conf. (GLOBECOM)*, Dec. 2010.

[20] Y. Wang, X. Cao, Q. Hu, and Y. Pan, "Towards elastic and fine-granular bandwidth allocation in spectrum-sliced optical networks," *J. Opt. Commun. Netw.*, vol. 4, no. 11, pp. 906–917, Nov. 2012.

[21] T. Takagi, H. Hasegawa, K. Sato, Y. Sone, B. Kozicki, A. Hirano, and M. Jinno, "Dynamic routing and frequency slot assignment for elastic optical path networks that adopt distance adaptive modulation," in *Optical Fiber Communication Conf. (OFC)*, Mar. 2011.

[22] L. Velasco, M. Klinkowski, M. Ruiz, V. López, and G. Junyent, "Elastic spectrum allocation for time-varying traffic in flexgrid optical networks," *IEEE J. Sel. Areas Commun.*, vol. 31, no. 1, pp. 26–38, Jan. 2013.

[23] A. N. Patel, P. N. Ji, J. P. Jue, and T. Wang, "Defragmentation of transparent flexible optical WDM (FWDM) networks," in *Optical Fiber Communication Conf. (OFC)*, Mar. 2011, paper OTuI8.

[24] Y. Wang, J. Zhang, Y. Zhao, J. Zhang, J. Zhao, X. Wang, and W. Gu, "Path connectivity based spectral defragmentation in flexible bandwidth networks," *Opt. Express*, vol. 21, no. 2, pp. 1353–1363, Jan. 2013.

[25] X. Chen, J. Li, P. Zhu, R. Tang, Z. Chen, and Y. He, "Fragmentation-aware routing and spectrum allocation scheme based on distribution of traffic bandwidth in elastic optical networks," *J. Opt. Commun. Netw.*, vol. 7, no. 11, pp. 1064–1074, Oct. 2015.

[26] H. Beyranvand and J. A. Salehi, "A quality-of-transmission aware dynamic routing and spectrum assignment scheme for future elastic optical networks," *J. Lightwave Technol.*, vol. 31, no. 18, pp. 3043–3054, Sept. 2013.

[27] B. Wang and P. Ho, "Energy-efficient routing and bandwidth allocation in OFDM-based optical networks," *J. Opt. Commun. Netw.*, vol. 8, no. 2, pp. 71–84, Feb. 2016.

[28] S. Fujii, Y. Hirota, H. Tode, and K. Murakami, "On-demand spectrum and core allocation for reducing crosstalk in multi-core fibers in elastic optical networks," *J. Opt. Commun. Netw.*, vol. 6, no. 12, pp. 1059–1071, Nov. 2014.

[29] A. Muhammad, G. Zervas, and R. Forchheimer, "Resource allocation for space-division multiplexing: Optical white box versus optical black box networking," *J. Lightwave Technol.*, vol. 33, no. 23, pp. 4928–4941, Dec. 2015.

[30] M. Dzanko, M. Furdek, G. Zervas, and D. Simeonidou, "Evaluating availability of optical networks based on self-healing network function programmable ROADMs," *J. Opt. Commun. Netw.*, vol. 6, no. 11, pp. 974–987, Nov. 2014.

[31] S. Fujii, Y. Hirota, H. Tode, and T. Watanabe, "Dynamic spectrum and core allocation reducing costs of architecture on demand nodes," in *40th European Conf. Optical Communication (ECOC)*, Sept. 2014.

[32] S. Fujii, Y. Hirota, H. Tode, and T. Watanabe, "Dynamic spectrum and core allocation with spectrum region reducing costs of building modules in AoD nodes," in *16th Int. Telecommunications Network Strategy and Planning Symp. (Networks)*, 2014.

[33] M. Jinno, B. Kozicki, H. Takara, A. Watanabe, Y. Sone, T. Tanaka, and A. Hirano, "Distance-adaptive spectrum resource allocation in spectrum-sliced elastic optical path network," *IEEE Commun. Mag.*, vol. 48, no. 8, pp. 138–145, Aug. 2010.

[34] M. Garrich, N. Amaya, G. Zervas, P. Giaccone, and D. Simeonidou, "Power consumption analysis of architecture on demand," in *European Conf. Optical Communication (ECOC)*, Sept. 2012.

Shohei Fujii received his B.E. and M.E. degrees from Osaka University, Japan, in 2013 and 2015, respectively. He is a doctoral student in the Department of Information Networking, Graduate School of Information Science and Technology, Osaka University. His research interests include switching architecture and control plane in optical networks, with a focus on spectrum resource allocation for large-capacity optical networks.

Yusuke Hirota is a Member of the IEEE. He received his B.E., M.E., and Ph.D. degrees from Osaka University, Japan, in 2004, 2006, and 2008, respectively. He has been an assistant professor in the Graduate School of Information Science and Technology, Osaka University, since Oct. 2008. His research interests include routing and spectrum assignment, switching architecture in optical networks, multicasting, multimedia streaming systems, peer-to-peer communications, and autonomous networks. Dr. Hirota is a member of The Optical Society (OSA) and the Institute of Electronics, Information and Communication Engineers, Japan.

Hideki Tode is a Member of the IEEE. He received his B.E., M.E., and Ph.D. degrees in communications engineering from Osaka University, Japan, in 1988, 1990, and 1997, respectively. He was an assistant professor in the Department of Communications Engineering, Osaka University, beginning in Dec. 1991. In 1998 and 1999, he became a lecturer and associate professor in the Department of Information Systems Engineering, and in 2002, he moved to the Department of Information Networking, Graduate School of Information Science and Technology. Since 2008, he has been a professor in the Department of Computer Science and Intelligent Systems, Graduate School of Engineering, Osaka Prefecture University, Japan. His current research interests include QoS-aware network controls, future optical/wireless network architecture, and contents distribution/retrieval technologies. Dr. Tode is a senior member of the Institute of Electronics, Information and Communication Engineers, Japan.

Takashi Watanabe is a Member of the IEEE and a member of the IEEE Communications Society and the IEEE Computer Society. He received his B.E., M.E., and Ph.D. degrees from Osaka University, Japan, in 1982, 1984, and 1987, respectively. He joined the Faculty of Engineering, Tokushima University, Japan, in 1987, as an assistant professor and moved to the Faculty of Engineering, Shizuoka University, Japan, in 1990. He was a visiting researcher with the University of California, Irvine, from 1995 to 1996. He is currently a professor with the Graduate School of Information Science and Technology, Osaka University, Japan. His research interests include wireless networking, mobile networking, ad hoc networks, sensor networks, ubiquitous networks, intelligent transport systems, especially MAC, and routing. Dr. Watanabe is a member of the Information Processing Society of Japan (IPSJ), and the Institute of Electronics, Information and Communication Engineers, Japan (IEICE). He has served on many program committees for networking conferences, such as the IEEE, the Association for Computing Machinery, IPSJ, and IEICE.